M. Koskenvuori and I. Tittonen, Towards micromechanical radio: overtone excitations of a microresonator through the nonlinearities of the second and third order, Journal of Microelectromechanical Systems, 17, pp. 363-369 (2008).

Towards Micromechanical Radio: Overtone Excitations of a Microresonator Through the Nonlinearities of the Second and Third Order

Mika Koskenvuori and Ilkka Tittonen

***Abstract*—A micromechanical resonator with eigenfrequencies in the megahertz-range is excited by signals having frequencies from tens of megahertz to gigahertz. The high-frequency excitation voltage is downconverted to mechanical force at the lower resonance frequency by the second-order force-voltage nonlinearity. The conversion is either assisted by additional local-oscillator signal or it is intrinsic due to an amplitude-modulated (AM) input signal. A circuit-simulator model is tested against measurements and an excellent agreement and thorough interpretation of the results is found. The third-order intercept point is measured and simulated to study the strength of the capacitive third-order nonlinearity. Finally, various nonlinear contributions are compared and further improvements for the device are suggested based on the simulations. [2007-0050]**

***Index Terms*—Frequency conversion, microelectromechanical devices, mixers, modeling, nonlinearities, resonators.**

I. Introduction

MEMS COMPONENTS are finding applications in modern wireless communication systems. Usually, silicon-based resonators with the smallest feature sizes in the micrometer range possess mechanical resonances that are a few megahertz. This is appropriate for example in voltage-controlled oscillator applications, but communication using transmission frequencies in the megahertz range requires the use of meter-size $\lambda/4$-antennas. One solution is to use a radial bulk annular resonator [1], wine-glass [2], or disk [3] resonators at gigahertz-frequencies. However, because the mechanical impedance of the resonators usually increases with the decrease of its size, this increase in frequency leads to a higher impedance level that is difficult to match for coupling. For this reason the first logical task in a MEMS-based transceiver is to convert the signal from high communication frequency to the resonance frequency of the MEMS-device. This could be achieved with the aid of a local oscillator (LO) that is inside the transceiver [4], [5]. Another solution is to select the input signals so that nonlinear processes convert the signal from the high communication frequency down to the eigenfrequency of the resonator. A further advantage is that both these methods offer a possibility for filtering of the signal due to the high mechanical quality factor of the resonators. Despite the large number of published micromechanical mixers, all the devices exhibit a large conversion loss (CL) [4]–[9] or require significant LO power for effective conversion [10], thus making them inappropriate for low-power wireless communication. Studies have shown that parametric amplification can be an effective, active way to improve the conversion performance of micromechanical mixers by even 30 dB [11]. In this paper, further possible improvements in the conversion performance are studied by physical simulations. Before the improvements are presented, the current performance of the mixer is modeled with high accuracy using excitations of various orders to give credibility to and to justify the improved simulation results. The simulations are performed with a circuit simulator that, in addition to circuit level simulations that use the electrical equivalent components of a micromechanical resonator, is capable for mixed system and circuit level simulations. Because of this, the accurate simulations of the device performed here set an important background for future work where complete systems featuring micromechanical resonators as working blocks can be simulated.

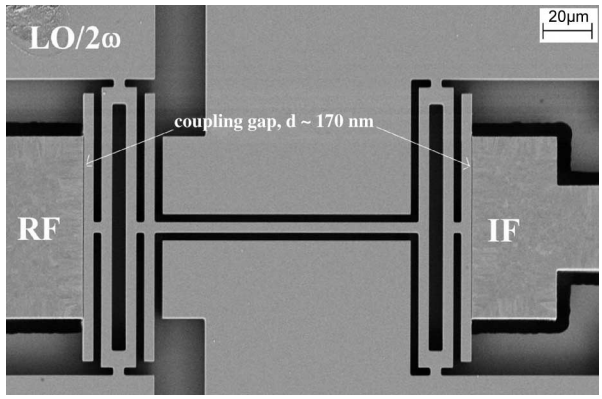

Fig. 1. SEM-view of the used DETF-resonator. The resonator is fabricated on SOI-wafer with deep reactive ion etching. The resonance mode frequency is $f_{\rm res} = 1.338$ MHz and the coupling gap is $d \approx 170$ nm in width. The labels RF, LO, and IF mark the corresponding electrodes used throughout the text.

II. Device Fabrication, Characterization and Modeling

The resonator used here is a double-ended tuning fork (DETF) resonator (Fig. 1) used previously in [9]. It was fabricated at the VTT Technical Research Centre of Finland. The coupling gap d was reduced from $d \approx 1$ μm to $d \approx 170$ nm

Manuscript received February 27, 2007; revised January 25, 2008. Subject Editor S. Lucyszyn.

The authors are with the Department of Micro and Nanosciences, Center for New Materials, Helsinki University of Technology (TKK), 02015 Espoo, Finland (e-mail: mika.koskenvuori@tkk.fi).

Color versions of one or more of the figures in this paper are available online at http://ieeexplore.ieee.org.

Digital Object Identifier 10.1109/JMEMS.2008.918376

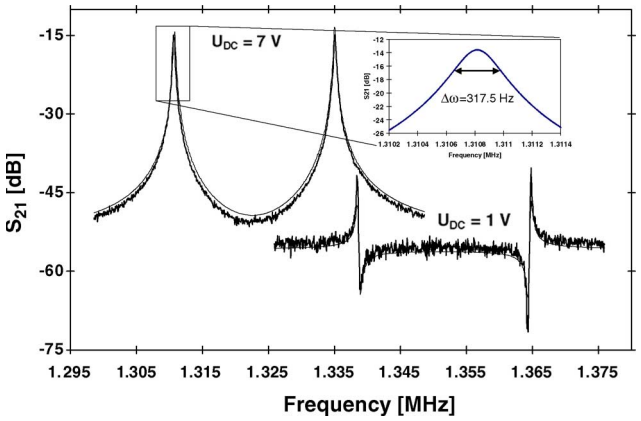

Fig. 2. Measured (thick lines) and simulated (thin lines) transmission responses of the resonator used. Here, $U_{\rm dc} = [1, 7]$ V is applied as a bias voltage on both RF- and IF-electrodes that are indicated in Fig. 1 and $P_{\rm ac} = -50$ dBm is applied on the RF-electrode for excitation. The responses are readout from the IF-electrode. The insert is zoomed on the first resonance showing the bandwidth of the resonance ($\Delta\omega = 317.5$ Hz) that can be used to calculate the Q-factor of the resonance, $Q \approx 4130$.

by depositing polycrystalline silicon [12]. The resonator was fabricated on an SOI-wafer with a device layer of thickness $h = 10$ μm. The length and the width of the tuning fork beam are $L = 100$ μm and $w = 5$ μm, respectively. The device utilizes two mechanically coupled tuning forks for the increased LO-IF and LO-RF isolation. The signals are coupled capacitively via the RF-contact pad and when necessary directly via the LO-contact pad depending on the mode of the application. The output is capacitively readout via the IF-pad with a FET preamplifier.

To characterize the relevant parameters of the resonator to generate an accurate model for the circuit simulator [13], transmission response (S_{21}) of the resonator with varying bias $(U_{\rm dc})$ voltages below the pull-in voltage were recorded (Fig. 2). In addition to the resonator, biasing and readout circuitry were also added into the model. The resonator was modeled as an electrical equivalent of the spring-mass system, and for the capacitive coupling a model taking into account the usual second-order force-voltage and also the third-order capacitive nonlinearity was used [14]. The parameters describing the mechanical (eigenfrequency $f_{\rm res}$, spring constant $k_{\rm mech}$, Q-value Q, coupling gap width d and the electrode length $L_{\rm e}$) and electrical parameters (pad and feed-through capacitances $C_{\rm pad}$ and $C_{\rm thr}$, respectively) were modeled using transient analysis by finding a best fit to the measurements with Nelder–Mead [15] optimization method. As the excitation was performed at low frequencies around the fundamental resonance frequency of the device $(f_{\rm res} \approx 1.3$ MHz) this analysis left some parameters open. For example the feed-through capacitances were modeled as one lumped capacitance. The accuracy of the model was increased by the direct-conversion (mixer) measurements at higher frequencies (Section III). The mixer-simulations were carried out using large-signal harmonic balance (HB) analysis utilizing multiple independent input and output tones (excitation frequencies) and their harmonics. Especially for devices with high quality factors and therefore long settling times, HB analysis (carried out in frequency domain) is very efficient when compared to transient analysis (carried out in time domain) [16].

At least three kinds of distinct nonlinearities are usable for mixing in capacitively coupled micromechanical devices [9]. Usually, the strongest contribution originates from the typical nonlinear dependence between the force and voltage across the transducer gap so that the actuating force F is related to the applied voltage U by a relation

$$F = \frac{1}{2}U^2\frac{dC}{dx}. \tag{1}$$

This is valid for the whole displacement amplitude range x. The other two nonlinear contributions arise as the displacement amplitude increases. For capacitive devices, the coupling capacitance depends on the displacement amplitude x in a nonlinear way according to

$$C(t) = \frac{A\varepsilon_0}{d \pm x(t)} = \frac{L_{\rm e}h\varepsilon_0}{d \pm x(t)} \tag{2}$$

where $L_{\rm e}$ and h are the length and height of the transducer electrode, respectively and d is the coupling gap. Eventually, the capacitive nonlinearity will limit the maximum attainable vibration amplitude [17], but with vibration amplitudes lower than this, the capacitive nonlinearity can be interpreted as softening of the mechanical spring thus effectively lowering the resonance frequency (Fig. 2).

The capacitive nonlinearity does not usually limit the operation of the resonator when the displacement amplitude x is small when compared to the coupling gap d and (2) can be written as $C \approx C_0/d$, where C_0 is the capacitance in (2) with $x = 0$. However, as can be seen in Section V, capacitive nonlinearity is a significant source of intermodulation (IM) distortion especially because the high electromechanical coupling with narrow coupling gaps is usually preferred.

For a device measured here, mechanical nonlinearity is not significant because the displacement amplitudes on the order of $x = 10$ nm are negligible when compared to the length of the resonating beam $L = 100$ μm [17].

III. Mixer (Direct Conversion) Results

Force-voltage nonlinearity combined with a sharp resonance ($Q > 4000$, corresponding to 3 dB bandwidth < 320 Hz) makes micromechanical resonators potential candidates for combined mixer-filter applications [4]–[10]. If two signals $U_{\rm RF}(t) = \hat{U}^*_{\rm RF}\sin[(\omega_{\rm LO} + \omega_{\rm res})t]$ and $U_{\rm LO}(t) = \hat{U}^*_{\rm LO}\sin[(\omega_{\rm LO})t]$ are applied to the resonator, it can be calculated from (1) that the resulting force will have a component at frequency $\omega_1 - \omega_2 = \omega_{\rm res}$. This can be measured and simulated with an RF-signal coupled to the RF-electrode and a LO-signal coupled to the LO-electrode. The down-converted signal can be detected from the IF-electrode with the aid of dc bias voltage. In the frequency domain, this can be depicted as Fig. 3(a) To characterize the device at both low and high carrier frequencies, the conversion was measured at three different LO-signal frequencies, $f_{\rm LO} = [10, 100, 390]$ MHz with RF-signal at $f_{\rm RF} = f_{\rm LO} + f_{\rm res}$ or $f_{\rm RF} = [11.338, 101.338, 391.338]$ MHz,

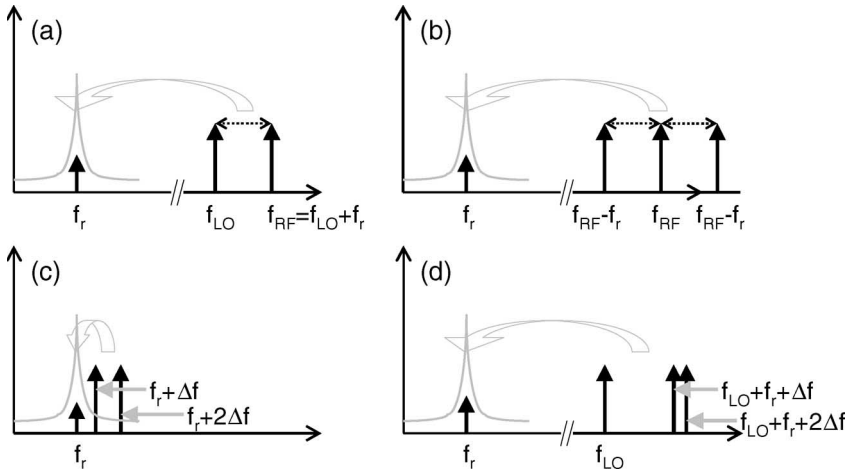

Fig. 3. Different conversion results from the nonlinearities of MEMS. (a) High-frequency signal converted with the aid of LO-signal. (b) AM-modulated high frequency signal converted intrinsically without LO-signal. (c) Third-order IM (because of capacitive nonlinearity) converts interfering signals outside the passband of a filter into the passband. (d) Same, but with a high-frequency interferers converted with the aid of LO-signal and third-order capacitive nonlinearity.

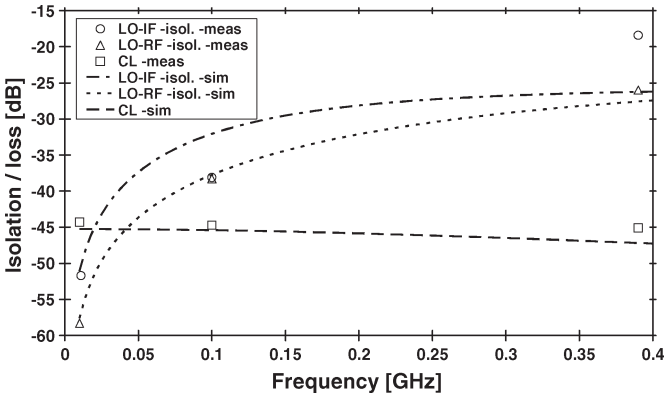

Fig. 4. Measured and simulated CL (rectangles), LO-IF—isolation (circles) and LO-RF—isolation (triangles). The model gives excellent quantitative match even up to 400 MHz, except for the LO-IF—isolation where the model and the measurements agree qualitatively. The isolations were measured with a 50 Ω termination at the input and output of the device.

where $f_{\rm res}$ is the frequency of the first resonance of the device (Fig. 2).

The measured and simulated results with an LO-signal power $P_{\rm LO} = 0$ dBm, an RF-signal power $P_{\rm RF} = -60$ dBm and a bias voltage $U_{\rm dc} = 7$ V are shown in Fig. 4.

The high CL includes the insertion loss and can be explained by the weak coupling of both RF- and LO-signals as the impedance of the resonator is much higher than 50 Ω. With proper impedance matching, which will become feasible when the coupling gap d can be fabricated to be lower than $d < 100$ nm, the performance of the mixer will be improved. This will be shown in Section VI.

IV. AM-Modulated Signal Down Conversion

A different approach in the excitation signal is needed if one wants to convert the excitation voltage down to a force at the resonance frequency of the device without any LO. Instead of applying a signal with a single frequency component, a signal with multiple frequency components with a separation equal to the resonance frequency of the resonator is used [8]. A good candidate for this approach is a high-frequency carrier signal that is AM by the resonance frequency of the device.

This approach can be written as

$$\begin{aligned} U(t) &= [A_0 + B_0\cos(2\pi f_{\rm m}t)]\cos(2\pi f_{\rm c}t) \\ &= A_0\left[\cos(2\pi f_{\rm c}t) + \frac{h}{2}\cos(2\pi f_{\rm c} \pm 2\pi f_{\rm m})t\right] \end{aligned} \quad (3)$$

where A_0 and B_0 are the amplitudes of the carrier and the modulation signal, respectively. $f_{\rm c}$ is the carrier frequency and $f_{\rm m}$ the modulation frequency, which is also the resonance frequency $f_{\rm res}$ of the resonator. Modulation index h is defined as $h = B_0/A_0$.

The down-conversion of the signal is done in the capacitive coupling gap, where the actuating force F is related to the applied voltage U by (1). This nonlinear relation ensures that the arising force F has a component also at the resonators resonance frequency $f_{\rm res} = f_{\rm m}$

$$F|_{f=f_{\rm m}}\left(\frac{1}{4}A_0^2h + \frac{1}{4}A_0^2h\right)\frac{dC}{dx} = \frac{1}{2}A_0B_0\frac{dC}{dx} \quad (4)$$

where $\partial C/\partial x$ is the electromechanical coupling factor. From (4), it is clear that it is convenient to have $A_0 = B_0$ or $h = 1$ as these factors contribute equally to the force. In the frequency domain, this can be depicted as Fig. 3(b).

To study the excitation of the resonator using gigahertz-range signal, an AM-modulated gigahertz-range carrier signal was generated. This signal was coupled to the resonator via the RF-electrode and the signal at frequency $f_{\rm m}$ was recorded from the IF-electrode with the aid of a dc-bias voltage $U_{\rm dc} = 7$ V. The resonator was grounded via the LO-electrode.

Fig. 5 shows the measured and simulated output signal ($V_{\rm out}$) of the resonator actuated with a modulated gigahertz-range signal ($V_{\rm in}$, $f_{\rm c} = [0.5, 1.5]$ GHz). It indicates a successful excitation of a megahertz-range resonator ($f_r = f_{\rm m} = 1.338$ MHz) with a gigahertz-range signal.

The weakness of the output signal can be partially explained by very weak coupling of the input signal as was the case in the

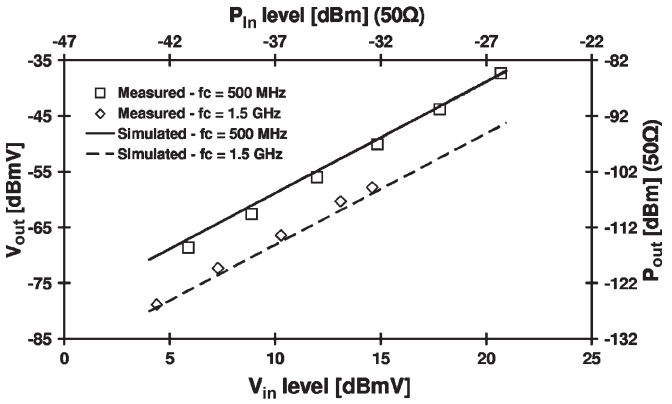

Fig. 5. Output signal voltage $V_{\rm out}$ as a function of input signal voltage $V_{\rm in}$. The figure indicates a successful excitation of megahertz-range resonator with gigahertz-range signal as the carrier frequency of the excitation signal is $f_{\rm in} = [0.5, 1.5]$ GHz and the recorded output signal frequency $f_{\rm out} = f_{\rm m} = 1.338$ MHz.

direct conversion mode. An additional explanation comes from (4) as the force at the resonance frequency is the product of two fairly small ac-signals, the strong LO-signal being absent. Again, by reducing the coupling gap d and with impedance matching the performance can be increased as shown in Section VI.

V. IM

The experiments done in the previous sections rely only on the second-order force-voltage nonlinearity. As described in Section II, other nonlinearities also exist in capacitively coupled micromechanical devices. The third-order nonlinearity that arises from the capacitive coupling brings IM distortion into the system even when the vibration is in the linear regime [17]. This can be seen by Taylor's expansion of the capacitance in (2)

$$C(t) = C_0 \left(1 \mp \frac{x(t)}{d} + \left(\frac{x(t)}{d}\right)^2 \mp \left(\frac{x(t)}{d}\right)^3 + \dots\right). \quad (5)$$

The IM distortion is responsible for converting the off-resonance signals into the resonance band. This is especially harmful in the case of filter-applications where those signals that are outside the filter passband would be converted inside the passband through the IM [Fig. 3(c)].

To quantify the strength of capacitive nonlinearity, a parameter called the third-order intercept point (IIP3) can be measured. It is a measure of how strong off-resonance interferers at frequencies ω_1 and ω_2 are needed to produce an equally strong signal in the carrier frequency as if the same power was applied directly at the carrier frequency.

In practice, if two signals at frequencies $\omega_1 = \omega_{\rm res} + \Delta\omega$, $\omega_2 = \omega_{\rm res} + 2\Delta\omega$ are applied to the RF-electrode of the resonator and the input and output electrodes are dc-biased, the cubic mixing of these signals produces in addition to other contributions a third-order term at frequency $2\omega_1 - \omega_2$, which is identified as $\omega_{\rm res}$. This process of the third-order IM distortion (IM3) product generation is depicted in the frequency domain in Fig. 3(c). IIP3 can be determined by extrapolating the linear-regime of the IM3 product [Fig. 6(a)] (solid lines).

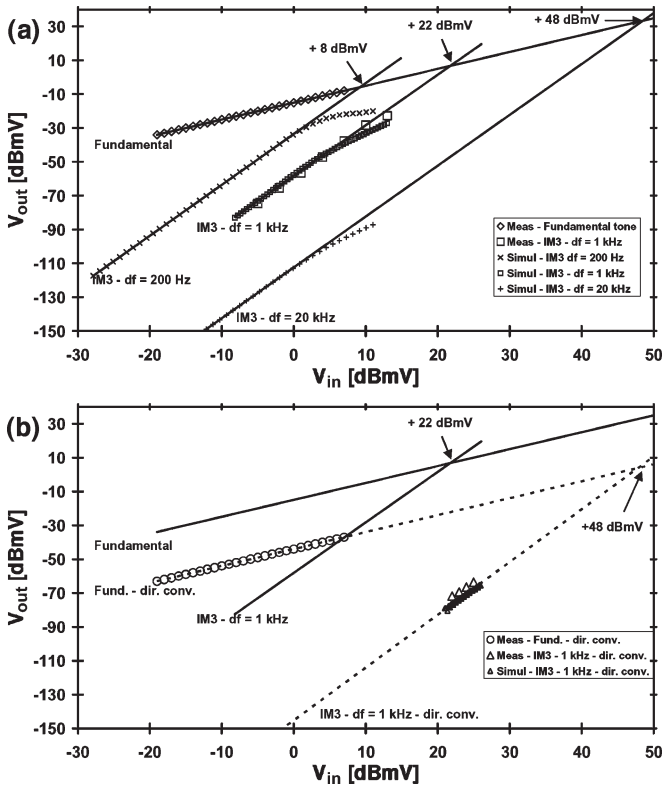

Fig. 6. Measured (big symbols) and simulated (small symbols) IIP3. (a) Measured response of the resonator in transmission mode for the fundamental tone (diamonds) and simulated results for two off-resonance tones spaced from resonance by $\Delta f = [200, 1000, 20\,000]$ Hz are depicted. To verify the model, IM3 was measured (squares) at $\Delta f = 1$ kHz excitation signal with excellent agreement. As expected, the near resonance tones produce stronger IM. The lines are extrapolations of the data used to determine IIP3. (b) For direct-conversion approach the fundamental response (circles) and both measured and simulated responses to interferers (triangles) at $\Delta f = 1$ kHz are shown. For direct conversion, the LO amplitude and frequency are $V_{\rm LO} = 47$ dBmV and $f_{\rm LO} = 11$ MHz. The dashed lines are extrapolations of the responses in the direct-conversion mode and the solid lines are extrapolations for transmission mode repeated here for reference.

Reference [18] reports a simple expression for calculating the IIP3 when the interferers lie inside the mechanical passband of the resonator. Using this formula, an IIP3 of $+2.3$ dBmV can be calculated for in-band interferers for the resonator studied here. The analytical result is slightly lower than the measured and simulated IIP3 of $+8$ dBmV, but the accuracy is comparable with the accuracy shown in [18] (analytical $+34.3$ dBmV versus simulated $+38$ dBmV). It should be noted that the IIP3 for the measured resonator is fairly low. It has been shown [18]–[20] that the IM3 is mainly generated due to the capacitive nonlinearity associated with the capacitive transduction and that there is a clear tradeoff between the linearity and the motional resistance of a device. The situation can be somewhat improved by increasing the mechanical spring constant with respect to the electrical spring. However, by careful selection of the vibration mode of the resonator and accepting the increased mechanical impedance, $R_{\rm m}$, signal-to-interference ratio values capable of meeting the Global System for Mobile Communications specifications can be reached with capacitive devices [19].

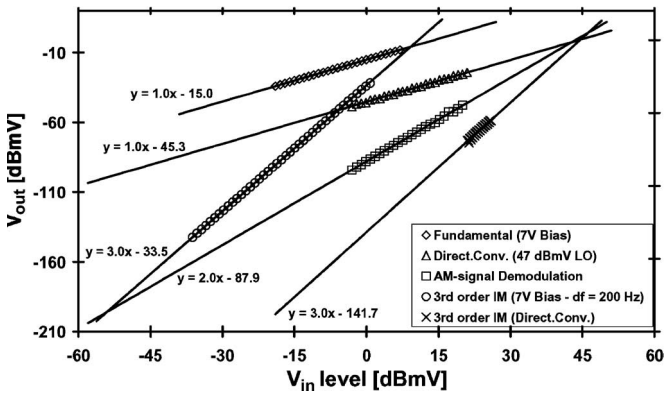

Fig. 7. Comparison between the different nonlinear phenomena studied in this paper. Of the nonlinear processes, the direct conversion mode results in the highest output signal at low input voltage levels ($V_{\rm in} < -10$ dBmV). Data points are from the simulations and lines are linear fits to the simulated data. Equations of the lines are given to visualize the order of each phenomenon.

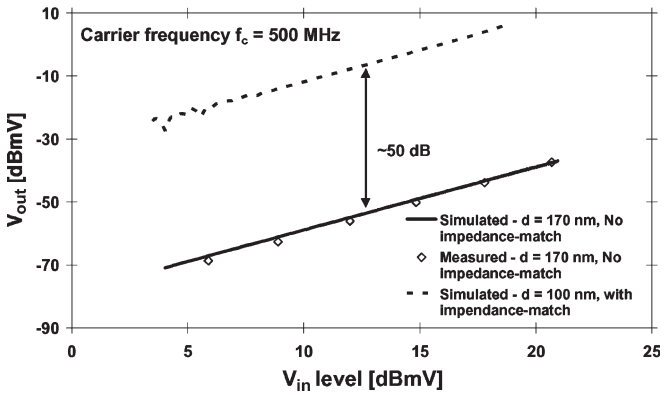

Fig. 8. Impedance match and the reduction of bonding pad capacitances increase the performance of AM-modulated signal down-conversion by almost 50 dB.

TABLE I
CONVERSION PERFORMANCE IMPROVEMENTS WITH IMPEDANCE MATCHING

		Measured device	Improved device
d	[nm]	170	100
U_{DC}	[V]	7	7
Z-match		No	Yes
C_{pad}	[pF]	4.9	0.049
f_{IF}	[MHz]	100	100
CL	[dB]	44	8
LO-IF isol.	[dB]	30	29
LO-RF isol.	[dB]	38	35

The IIP3 for the direct conversion (mixer-filter) mode can also be determined. For this approach, signals at frequencies $\omega_1 = \omega_{\rm LO} + \omega_{\rm res} + \Delta\omega$ and $\omega_2 = \omega_{\rm LO} + \omega_{\rm res} + 2\Delta\omega$ are summed and applied to the RF-electrode, and the signal at frequency $\omega_3 = \omega_{\rm LO}$ is applied to the LO-electrode. This is depicted in the frequency domain in Fig. 3(d). The IM3 product at frequency $\omega_{\rm res}$ is recorded from the IF-electrode. Simulations will become quite complicated as they require three independent tones ($\omega_{\rm res}$, $\Delta\omega$ and $\omega_{\rm LO}$) and up to five harmonics but results agree well with measurements as can be seen from Fig. 6(b) (dashed lines).

VI. DISCUSSION AND IMPROVEMENTS

To compare the three nonlinear processes, the relations between the output and the input voltages for different excitation schemes are plotted into the same figure (Fig. 7). The direct conversion mode can be considered as a first-order phenomenon because the output voltage is directly proportional to the input voltage or $U_{\rm out} \propto U_{\rm in}$. From (4) and by inserting (5) into (1), the demodulator and IIP3 can be seen to be second- and third-order phenomena, respectively. For low input voltages ($V_{\rm in} < -10$ dBmV), the direct conversion mode results in the highest output level when considering the nonlinear processes. This can be expected due to the strong LO signal used in this mode. Fig. 7 also emphasizes the current problem of poor conversion performance with micromechanical mixers. This can be seen from the constant term of the equations of the linear fits. The behavior is primarily due to the weak coupling of the electrical input signals to the mechanical resonator with high equivalent impedance and is a significant problem when aiming for low-power devices.

TABLE II
COMPARISON OF THE PRESENTED PERFORMANCE WITH PREVIOUSLY PUBLISHED RESULTS

Device	CL [dB]	P_{LO} [dBm]	f_{IF} [MHz]	f_{RF} [MHz]
This work	45 44	0	1.3	400 100
This work – improved[3]	8	0	1.3	100
DETF [9]	48	0	0.743	10
Two DETFs [9]	54	0	0.660	10
Cantilever [4]	39	13	0.435	400
C-c[1] beam [5]	75	5	22.5	1000
C-c[1] beam [6]	125	10	220	232
Coupled c-c[1] beams [10]	13	15	37	242
Coupled ring-resonators [7]	83.5	27	423	438
This work – AM modulated	70[4] 62[4]	N/A[2]	1.3	1500 500
This work – AM improved[3]	15[4]	N/A[2]	1.3	500
ADEX-10L[5]	8	4	800	1500

[1] Coupled-coupled or bridge resonator.
[2] Input signal is AM-modulated therefore no local oscillator is used in downconversion.
[3] Coupling and efficiency improvement studied using a circuit simulator.
[4] For an AM-modulated signal down-conversion, the conversion loss is proportional to the input signal power (5) due to the multiplication of the spectral components. Value presented here is then the power of all the spectral components is P_{in} = -30 dBm.
[5] Surface-mountable macroscopic diode-ring mixer

To reach a good performance, the coupling of the input signals to the resonator must be improved. The impedance matching will become feasible once the coupling gap d can be fabricated to be lower than $d < 100$ nm. The reduction of the coupling gaps will also enable the use of voltages closer to pull-in–voltage to strengthen the output signal pickup. As shown in the previous sections, the model is able to give an excellent match with a number of different measurements even in the case of complicated nonlinear phenomena. Encouraged

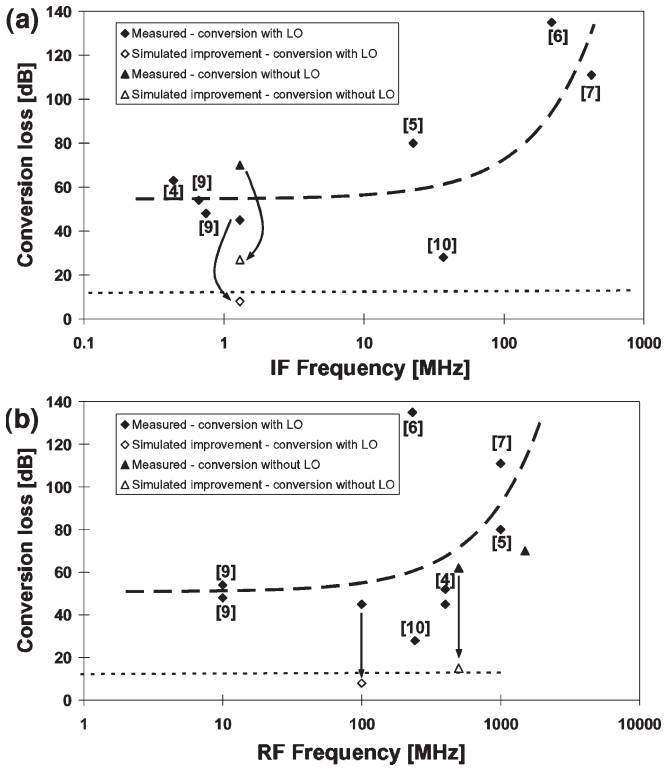

Fig. 9. CLs of some published micromechanical mixer-filters from Table II as a function of (a) IF- and (b) RF-frequency. For a justified comparison, all the CLs were normalized to a LO power of $P_{\mathrm{LO}} = 0$ dBm. The dashed line is a linear fit to the data to emphasize the degradation of the performance with increased frequency. The dotted line represents a conversion performance of a commercial surface mountable mixer (ADEX-10L) given as a reference. The arrows indicate the possible improvements that have been suggested though simulations.

by this, the accurate model was further used to probe the possibilities of the resonator. This was done by reducing the coupling gap to $d = 100$ nm while maintaining the bias-voltage $U_{\mathrm{dc}} = 7$ V bringing the system very close to pull-in ($U_{\mathrm{pi}} = 7.5$ V). Also, the bonding pad capacitances that are necessary for measurements but which can be greatly diminished for an actual integrated device were reduced from $C_{\mathrm{pad}} = 4.9$ pF to $C_{\mathrm{pad}} = 49$ fF.

For the direct conversion mode, the results can be seen in Table I. Table I indicates that with impedance matching a reasonable RF to IF conversion ratio can be achieved. From Fig. 8, the performance of the demodulator can be seen to improve almost 50 dB with the similar changes [8].

Table II and Fig. 9 summarize the results of the study and present a comparison with previously published micromechanical mixers. From Table II and Fig. 9, it is clear that micromechanical mixers exhibit large CLs when compared with conventional macroscopic mixers, but the simulation results shown here indicate that by careful design and fabrication of the resonant micromechanical mixers, their conversion performance can be brought to a level that is comparable with conventional devices. This way, the benefits of integrability, combined mixing and filtering and smaller size can be fully taken advantage of. However, due to the low resonant frequency and high quality factor of the presented devices, the data transmission rate would be moderate at the best. Therefore, future work should also concentrate on demodulating more sophisticated modulation schemes than AM.

Finally, it should be noted that the excellent match of the measurement and modeling results presented in this paper even in the case of nonlinear, high frequency multitone excitations indicates that a circuit simulator fitted with MEMS-component equivalents is a powerful tool in the analysis and design of microelectromechanical systems. When using a circuit simulator that also offers the possibility of incorporating circuit level simulations inside the system level simulations, MEMS components can be simulated as a part of a radio system enabling the development and simulation of a whole radio in terms of for example bit-error rate.

ACKNOWLEDGMENT

The authors would like to thank J. Kiihamäki for the microresonators used in the measurements and A. T. Alastalo for discussions.

REFERENCES

[1] B. Bircumshaw, G. Liu, H. Takeuchi, K. Tsu-Jae, R. Howe, O. O'Reilly, and A. Pisano, "The radial bulk annular resonator: Towards a 50 Ω RF MEMS filter," in *Proc. Tech. Dig. Transducers*, Boston, MA, Jun. 8–12, 2003, pp. 875–878.

[2] X. Yuan, L. Sheng-Shian, L. Yu-Wei, R. Zeying, and C.-T. C. Nguyen, "UHF micromechanical extensional wine-glass mode ring resonator," in *IEDM Tech. Dig.*, Washington, DC, Dec. 8–10, 2003, pp. 39.2.1–39.2.4.

[3] J. Wang, Z. Ren, and C. T.-C. Nguyen, "1.156-GHz self-aligned vibrating micromechanical disk resonator," *IEEE Trans. Ultrason., Ferroelectr., Freq. Control*, vol. 51, no. 12, pp. 1607–1628, Dec. 2004.

[4] F. Chen, J. Brotz, U. Arslan, C.-C. Lo, T. Mukherjee, and G. K. Fedder, "CMOS-MEMS resonant RF mixer-filters," in *Proc. IEEE MEMS*, 2005, pp. 24–27.

[5] A. Uranga, J. Verd, J. L. Lopez, J. Teva, G. Abadal, F. Torres, J. Esteve, F. Perez-Murano, and N. Barniol, "Fully integrated MIXLER based on VHF CMOS-MEMS clamped-clamped beam resonator," *Electron. Lett.*, vol. 43, no. 8, pp. 452–454, Apr. 2007.

[6] J. L. Lopez, J. Teva, A. Uranga, F. Torres, J. Verd, G. Abadal, and N. Barniol, "Mixing in a 220 MHz CMOS-MEMS," in *Proc. IEEE ISCAS*, New Orleans, LA, May 27–30, 2007, pp. 2630–2633.

[7] S.-S. Li, Y.-W. Lin, Y. Xie, Z. Ren, and C. T. C. Clark, "Small percentage bandwidth design of a 423-MHz notch-coupled micromechanical mixler," in *Proc. IEEE Ultrasonics Symp.*, 2005, pp. 1295–1298.

[8] M. Koskenvuori and I. Tittonen, "GHz-range FSK-reception with microelectromechanical resonators," *Sens. Actuators A, Phys.*, vol. 142, no. 1, pp. 346–351, Mar. 2008.

[9] A. T. Alastalo, M. Koskenvuori, J. Kiihamäki, and H. Seppä, "A micromechanical resonating RF mixer," in *Proc. EuMW*, Amsterdam, The Netherlands, Oct. 12–14, 2004, pp. 1297–1300.

[10] A.-C. Wong and C. T.-C. Nguyen, "Micromechanical mixer-filters ('Mixlers')," *J. Microelectromech. Syst.*, vol. 13, no. 1, pp. 100–112, Feb. 2004.

[11] M. Koskenvuori and I. Tittonen, "Improvement of the conversion performance of a resonating multi-mode microelectromechanical mixer-filter through parametric amplification," *IEEE Electron Device Lett.*, vol. 28, no. 11, pp. 970–972, Nov. 2007.

[12] J. Kiihamäki, V. Kaajakari, H. Luoto, H. Kattelus, and M. Ylikoski, "Fabrication of single crystal silicon resonators with narrow gaps," in *Proc. Tech. Dig. Transducers*, Seoul, Korea, Jun. 5–9, 2005, pp. 1354–1357.

[13] *Aplac RF Design Tool*, AWR-APLAC Corp., Espoo, Finland. [Online]. Available: www.aplac.com

[14] T. Veijola and T. Mattila, "Modelling of nonlinear micromechanical resonators and their simulation with the harmonic-balance method," *Int. J. RF Microw. Comput.-Aided Eng.*, vol. 11, no. 5, pp. 310–321, Sep. 2001.

[15] S. Maas, *Nonlinear Microwave and RF-Circuits*, 2nd ed. Norwood, MA: Artech, 2003.

[16] W. Press, B. Flannery, S. Teukolsky, and W. Vetterling, *Numerical Recipes in C*. Cambridge, U.K.: Cambridge Univ. Press, 1990.

[17] V. Kaajakari, T. Mattila, A. Oja, and H. Seppä, "Nonlinear limits for single-crystal silicon microresonators," *J. Microelectromech. Syst.*, vol. 13, no. 5, pp. 715–724, Oct. 2004.
[18] A. T. Alastalo and V. Kaajakari, "Intermodulation in capacitively coupled microelectromechanical filters," *IEEE Electron Device Lett.*, vol. 26, no. 5, pp. 289–291, May 2005.
[19] A. T. Alastalo and V. Kaajakari, "Third-order intermodulation in microelectromechanical filters coupled with capacitive transducers," *J. Microelectromech. Syst.*, vol. 15, no. 1, pp. 141–148, Feb. 2006.
[20] R. Navid, J. R. Clark, M. Demirci, and C. T.-C. Nguyen, "Third order intermodulation distortion in capacitively driven CC-beam micromechanical resonators," in *Proc. Tech. Dig. 14th Int. IEEE Micro Electro Mech. Syst. Conf.*, Interlaken, Switzerland, Jan. 21–25, 2001, pp. 228–231.

Mika Koskenvuori received the M.Sc. degree in electrical engineering from Helsinki University of Technology (TKK), Espoo, Finland, in 2002, where he has been working toward the Ph.D. degree at the Department of Micro and Nanosciences Laboratory.

Since then he has been working as a Research Scientist at the TKK, Espoo, Finland. His main research interests are RF-micromechanics and microsystems.

Ilkka Tittonen received the M.Sc. and Dr. Tech. degrees from the Department of Technical Physics, Helsinki University of Technology (TKK),Espoo, Finland, in 1988 and 1992, respectively.

The years 1995 to 1997, he worked as the Alexander von Humboldt stipendiat at the University of Konstanz, Germany. Then, he joined the Metrology Research Institute of Helsinki University of Technology as the Senior Assistant. Since the beginning of the year 2001, he has been appointed as the Professor of Physics at TKK. Currently, he has been with the Department of Micro and Nanosciences Laboratory. His current research interests are microsystems, nanotechnology, and atom optics.